Texture, 1972, Vol. 1, pp. 117–123.

ANISOTROPY IN SOME SOFT MAGNETIC MATERIALS

W. B. HUTCHINSON and J. G. SWIFT

Department of Physical Metallurgy, University of Birmingham, Edgbaston, Birmingham 15, *England; and West Midland Gas Board, Solihull, England*

(*Received March* 20, 1972, *in final form June* 9, 1972)

Orientation distribution data are presented for low carbon steel and silicon iron after different rolling and annealing schedules. Magnetic properties which depend solely on orientation can be well described using such distributions. A general analysis is demonstrated by which other properties may be divided into two components which are respectively dependent and independent of orientation. An example of this, a.c. power loss, is considered in detail. It is shown that the orientation-dependence of power loss derives entirely from the hysteresis component. The classical eddy current loss together with an 'anomalous' loss of similar magnitude constitute the orientation-independent part. The analysis may be used to predict properties under a range of conditions in textured materials.

INTRODUCTION

A very important commercial application of texture in metals lies in materials for electrical transformer cores and other electro-magnetic operations. For many years, the standard material for core laminations of power transformers has been $3\frac{1}{4}\%$ silicon steel treated to exhibit a very strong (110)[001] orientation, or Goss texture.[1] This grain oriented structure is produced by secondary recrystallisation and has a grain size in the range 3 to 10 mm in the plane of the sheet, which is typically 0.3 mm thick. The good magnetic properties of this material are largely due to the fact that the easy directions of magnetisation ⟨001⟩ in the different grains are aligned along a single direction in the sheet.

Power losses during alternating magnetisation of transformer cores have several origins. There is the classical eddy current loss[2] which depends most strongly on resistivity and sheet thickness, and is essentially independent of orientation. Conversely, the static hysteresis loss is very strongly dependent on the direction of magnetisation. Finally, there is the so called anomalous loss for which several explanations have been suggested. Micro eddy currents and damping effects at moving domain boundaries have been proposed by Pry and Bean[3] and Lee[4] as origins of the anomaly. However, Overshott *et al.*[5] also consider that domain boundary bowing at the free surfaces of thin sheet is an additional contribution. Despite the importance of preferred orientation to the magnetic properties, there has been rather little direct evidence published concerning the relationships. McCarty *et al.*[6] found that permeability and power loss were most strongly affected by rotational deviations from the ideal (110)[001] orientation around the sheet plane normal. Misorientations around axes perpendicular to this were not found to influence the properties strongly. However, a contrary observation was made by Daniels[7] who found that large rotational deviations around the transverse direction caused high power losses. It may be remarked that rotations around the normal and transverse directions are crystallographically identical but, because of the two dimensional nature of the grain structure, these may cause different magnetic closure domain structures. From a practical viewpoint, the Goss textured silicon steel is awkward to examine for preferred orientation. The grain size is too large for pole figure determination by x-ray analysis, and grain by grain measurements using Laue or etch pit methods are extremely time consuming.

Generally speaking, one may divide magnetic properties into those which are dependent on both orientation and microstructure (e.g. power loss), and those which depend solely on orientation. Examples of the latter type are the magnetostatic energy at saturation and the magnetic torque, which is the differential of that energy with respect to angular displacement. The torque magnetometer has been widely used for testing preferred orientation of electrical steels for quality control. Analysis of torque curves is normally based on the equation for the magnetostatic energy E[8]

$$E = K_0 + K_1(l^2m^2 + m^2n^2 + n^2l^2) + K_2 l^2m^2n^2 \ldots \quad (1)$$

This is a rationalisation of symmetry considerations for a cubic crystal in which the magnetisation vector has the direction cosines l, m, n. The coefficients K_0, K_1, K_2 are termed magnetocrystalline anisotropy coefficients. Where shape anisotropy can be ignored, as for example in a thin disc whose plane includes the field direction, the differential of E with respect to angle gives the torque experienced by the sample. This can be readily measured. A solution of this differential for the K_1 term of a general orientation has been given by Tarasov and Bitter[9]. Usually subsequent terms are of little weight. Particular solutions for high symmetry orientations can be found in most text books of magnetic materials.

In order to apply the above type of analysis to a polycrystalline metal, one requires to know a distribution of the orientations present. This is not directly measurable but may be calculated from pole figure data using methods developed by Williams[10] or Bunge[11] and Roe[12]. Bunge[13] has also shown mathematically how a distribution function of orientations may be applied to calculate the magnetic torque behaviour of rolled sheet material.

Since the use of orientation distributions is rather new, there is little complete data as yet published concerning texture in steels. Bunge[14] and Hutchinson and Swift[15] have given results for low carbon steel cold rolled 70%. The rolling texture is seen to consist primarily of a fibre texture with $\langle 111 \rangle$ parallel to the sheet normal and another with $\langle 110 \rangle$ along the rolling direction. There is a peak in the latter at approximately the orientation (223)[$\bar{1}$10]. Heckler and Granzow[16] have presented data at various reductions between 0% and 80%. These authors observed the (100)[011] orientation to be strongly populated at low reductions, but this may have been due to its presence in the starting texture. With continuing deformation the $\langle 111 \rangle$ and $\langle 110 \rangle$ fibre textures develop similar orientation densities, except for components in the latter fibre within 15° of (110)[$\bar{1}$10] which are suppressed. After annealing at 700°C, the $\langle 110 \rangle$ fibre texture is observed to become much depleted. There is also general agreement that the Goss orientation (110)[001] appears on primary recrystallisation.

EXPERIMENTAL

The work reported here was carried out on a low carbon rimming steel and a 1.8% silicon iron, the latter being of the type used commercially as low grade electrical steel. The rimming steel was cold rolled 50%, 70%, and 90% and a part of each was subsequently annealed at 700°C for one hour. Discs of 3 cm diameter were punched from these for torque magnetometer measurements. The silicon iron was first annealed for one hour at 1050°C and furnace cooled to form a coarse grain structure. This was followed by 60% cold reduction and a recrystallisation anneal of one hour at 700°C. Duplicate test specimens of dimensions 3 cm × 30 cm were cut with the long axes at angles of 0°, 15°, 30°, 45°, 60°, 75°, and 90° to the rolling direction. Finally, all the strip specimens were chemically polished to remove inhomogeneous surface layers and strained layers of the sheared edges.

Composite specimens of all the samples were made by soldering the sheets together and then 1.5 cm diameter spheres were machined from the composites. Complete (200) and (222) pole figures were obtained by the Jetter-Borie technique[17] from these spherical specimens. The pole figure data were also used to calculate three dimensional orientation distribution plots using the biaxial pole figure program of Williams.[10] This program gives solutions for the orientation density (t) at 1296 different orientations. The definition of angles used by Williams is given in Figure 1. One may also note that for a sheet plane orientation defined by the angles ρ and α, any direction lying in the plane defined by an angle β has direction cosines l, m, and n which are given by the relationships

$$l = \sin\beta\,(1-\sin^2\rho\,\sin^2\alpha)^{\frac{1}{2}} \tag{2}$$

$$m = -(\cos\rho\,\cos\beta+\sin^2\rho\,\sin\alpha\,\cos\alpha\,\sin\beta)/(1-\sin^2\rho\,\sin^2\alpha)^{\frac{1}{2}} \tag{3}$$

$$n = (\sin\rho\,\cos\alpha\,\cos\beta-\sin\rho\,\cos\rho\,\sin\alpha\,\sin\beta)/(1-\sin^2\rho\,\sin^2\alpha)^{\frac{1}{2}} \tag{4}$$

Hence, throughout the range of values of α, ρ, and β one can solve for the bracketed terms in Eq. (1).

Magnetic torque curves were obtained from the rimming steel samples using a conventional torsion-wire magnetometer. Measured values were corrected according to the specimen dimensions to express them as torque per unit volume.

The strips of silicon iron were tested for total power loss at 30, 50, and 60 Hz with a maximum induction of 1.0 tesla. In addition, complete B–H loops were measured using a d.c. permeameter for B_{max} equal to 1.0 tesla. From these graphs the

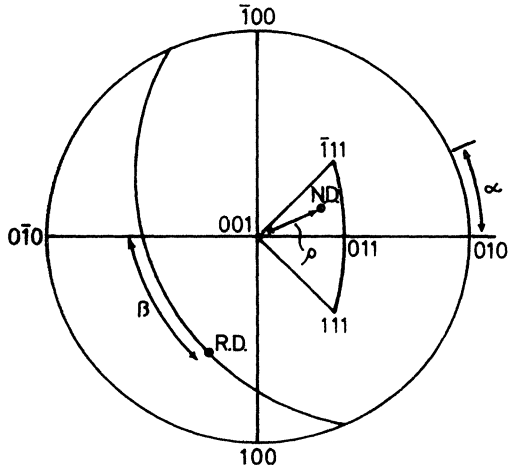

FIGURE 1 The definition of angular parameters.

remanence and coercive force were determined, and the hysteresis loss per cycle was calculated from the area of the loop.

RESULTS AND DISCUSSION

The orientation density plots for rimming steel cold rolled 50% and 90% are shown in Figures 2 and 3. That for the 70% reduction has been given previously.[15] It is clear that the texture is already well developed at 50% and at this stage it differs little in form from that at 90%. The main change which occurs with increasing reduction is strengthening of the major components at the expense of all other orientations. In particular, the density in orientations close to (223)[$\bar{1}$10] increases sharply and these become the strongest single components. The

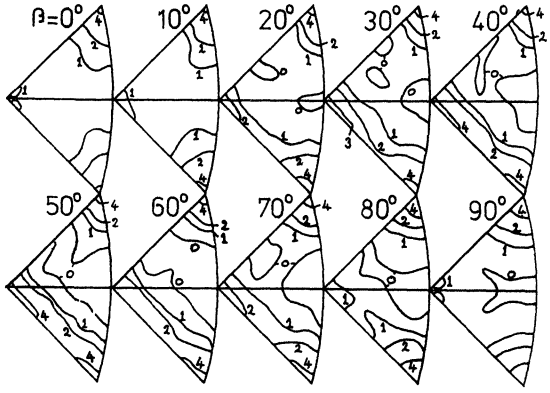

FIGURE 2 Biaxial pole figure for rimming steel rolled 50%.

orientation distributions after annealing at 700°C are shown in Figures 4 and 5. While the fibre texture with ⟨111⟩ along the normal direction is little affected by the heat treatment, that with ⟨110⟩ along the rolling direction is almost completely eliminated. The results of Bunge[14] at 70% reduction indicate a similar behaviour although in that case the ⟨111⟩ components were strengthened, while here they were observed to diminish somewhat. There is good qualitative agreement between the present observations and the theory of Dillamore *et al.*[18] which is based on a sub-grain growth model for nucleation of recrystallisation. Analyses based on oriented growth assuming 30° rotations around ⟨110⟩ poles are not successful in predicting most of the ennealing texture components.

In addition to the ⟨111⟩ orientations, there are two prominent annealing texture components. After low reduction the Goss component (110)[001] is very significant, while after heavy reduction there is strong component near (411)[14$\bar{8}$]. These are believed to derive from transition band and grain boundary nucleation sites respectively, and will be considered in detail elsewhere.[19,20] The orientation distribution for the silicon iron (Figure 6) is similar to the rimming steel (Figure 4) but has a stronger Goss component because of the coarser initial grain size employed.

In order to compute torque magnetometer curves for the polycrystalline structures, values were first calculated for the 1296 single orientations which are used for plotting the biaxial pole figures. To do this l, m, and n in Eq. (1) were expressed in terms of the angles α, ρ, and β, and the expression was differentiated with respect to β. Values of K_1 and K_2 were assumed to be 420×10^3 and 150×10^3 erg/cm^3 respectively.[21] An arithmetic mean of all the torque values was then taken after weighting the individual values by the orientation density factor t. A general texture component $\{hkl\}\langle uvw\rangle$ is represented in a sheet by four physically distinct orientations. For any single testing direction in the sheet plane, two of these behave identically and their properties are related to the other pair by reflection in the mirror planes of symmetry in the texture. Since the Williams representation, for economy of space, presents only one of the four components, a symmetry operation was performed to generate the properties of the missing variant.

Examples of the computed and measured torque curves are shown in Figures 7 and 8 for the 50% annealed and 90% rolled specimens. Results for the specimens after 70% reduction are given else-

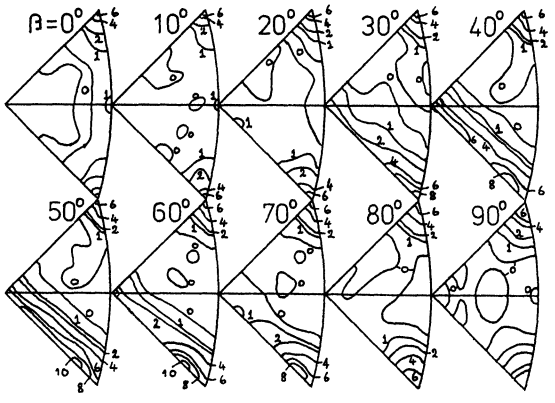

FIGURE 3 Biaxial pole figure for rimming steel rolled 90%.

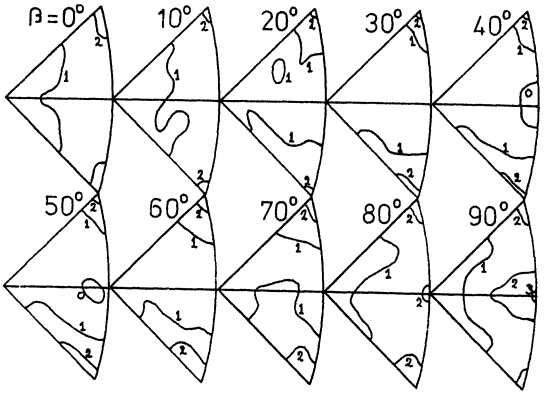

FIGURE 4 Biaxial pole figure for rimming steel rolled 50% and annealed at 700°C.

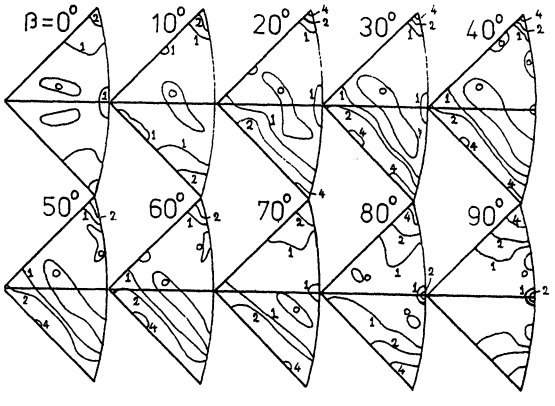

FIGURE 5 Biaxial pole figure for rimming steel rolled 90% and annealed at 700°C.

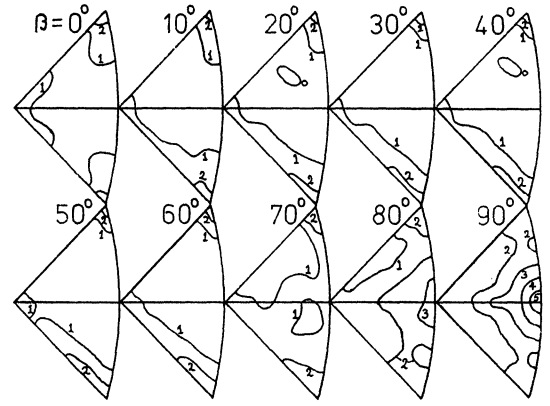

FIGURE 6 Biaxial pole figure for silicon iron rolled 60% and annealed at 700°C.

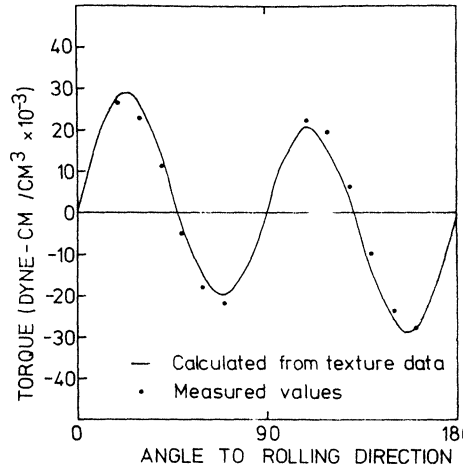

FIGURE 7 Torque magnetometer curve for rimming steel rolled 50% and annealed at 700°C.

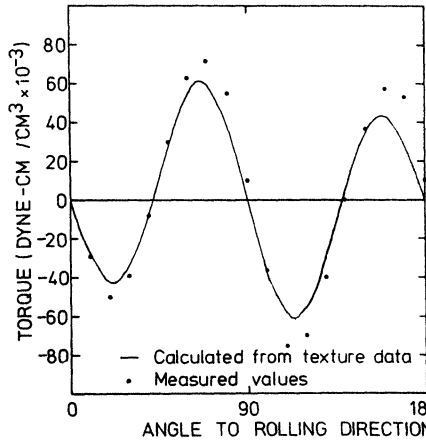

FIGURE 8 Torque magnetometer curve for rimming steel rolled 90%.

where.[15] Very close agreement is obtained in most cases, confirming the applicability of the method and the texture analysis. The 90% rolled specimen gives qualitative agreement, but quantitatively the results are not so good as in the other cases. It seems possible that here the texture is too sharp to be completely explained by the analysis used. Indeed, the discrepancies between measured and regenerated pole figures were noticeably larger than for the other specimens. At the lower reductions[15] the degree of fit is equally good for the cold worked and the recrystallised samples, and it is clear that the magnetocrystalline anisotropy coefficients are not significantly affected by deformation.

In the analysis of power loss and a number of other magnetic properties one requires to distinguish between contributions from crystal orientation, and those which derive from the microstructure. For cubic crystal symmetry, any directional property is capable of expression in series form as in Eq. (1). Provided that there are no interactions between grains, the value for a polycrystal may be obtained by averaging the single crystal values weighted by the orientation density of each. One can thus express a general property P as:

$$P = A_0 + A_1[(l^2m^2 + m^2n^2 + n^2l^2)t]_{Av} + A_2[(l^2m^2n^2)t]_{Av} + \ldots \quad (5)$$

where the average is carried out over a sufficiently large volume of orientation space. This approach has been outlined by Bunge[13] in relation to texture description using spherical functions. In the present work it was found that the bracketed terms for A_2 and higher orders were much smaller than that for $A_1 (< 5\%)$ and could reasonably be neglected. The physical property in question could then be described by the two coefficients A_0 and A_1, the former representing the orientation-independent part of the property and the latter representing its orientation-dependent part. Using direct measurements of the property in question along seven directions around the sheet and values of $[(l^2m^2 + m^2n^2 + n^2l^2)t]_{Av}$ calculated for the same directions from the orientation distribution, the values of A_0 and A_1 were obtained using a least squares solution.

Figure 9 shows the measured values of total power loss at three frequencies and the curves fitted to these using the texture data. It is seen that both coefficients A_0 and A_1 increase with frequency. A_1 varies almost linearly while A_0 shows a slightly stronger frequency dependence. The proportion of

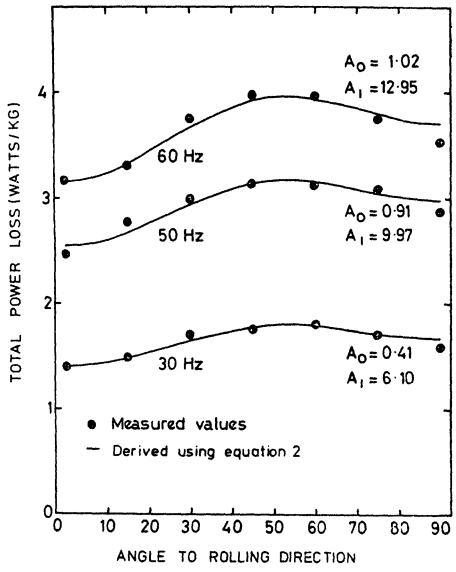

FIGURE 9 Total power loss data for the silicon iron.

the total power loss which is independent of texture is approximately 25% in this material. For ideally oriented sheets with the same microstructure and dimensions, the total loss would be simply equal to A_0 since the direction cosines expression would reduce to zero. This can thus provide a target at which to aim when developing textured steels for magnetic applications. Another application of the procedure described here is in the calculation of physical properties along directions where direct measurement is not possible. Knowledge of the orientation distribution and the coefficients A_0 and A_1 allows determination of the property along any direction in the polycrystalline aggregate.

In Figure 10, plots are presented of measured and derived values obtained from the static magnetisation curve. In the case of the hysteresis loss (B–H loop area), a small negative value of A_0 was found using the least squares analysis. Since this is physically unreasonable, the value of A_0 was set to zero which caused only a very small change in the A_1 term. Multiplying this loss/cycle value by the frequency gives the contribution of hysteresis to total power loss. Table I summarises these results and also the calculated classical eddy current losses.

Two important conclusions may be drawn from the data of Table I. Since the A_1 coefficients for total loss and hysteresis loss are the same within experimental error, then the orientation dependence of power loss is entirely due to the hysteresis contribution. Secondly, the classical eddy current loss

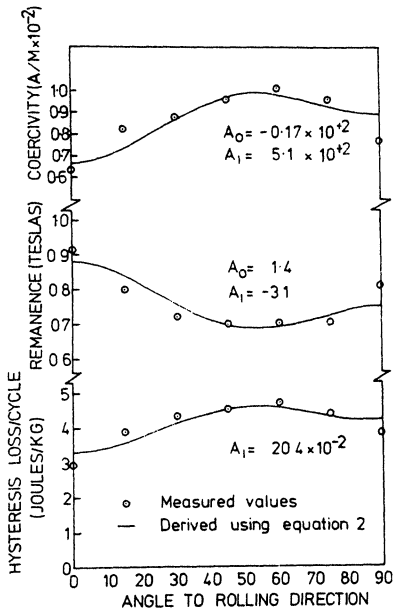

FIGURE 10 Permeameter results for the silicon iron.

is smaller than the term A_0 of the total power loss, indicating that there is an additional orientation-independent part of the power loss present. This additional term is of similar magnitude to that calculated from classical eddy current theory and is approximately proportional to frequency. It is possible that this loss derives from micro eddy current at moving domain boundaries, which was the mechanism suggested by Pry and Bean[3] to explain a similar magnetic anomaly.

TABLE I

Loss coefficients and calculated eddy current losses in units of watts/kg

Frequency	Total Power Loss Coefficients		Hysteresis Loss Coefficients		Classical Eddy Current Loss
	A_0	A_1	A_0	A_1	
30 Hz	0.41	6.10	0	6.1	0.14
50 Hz	0.91	9.97	0	10.2	0.37
60 Hz	1.02	12.95	0	12.2	0.54

In Figure 10, attempts were also made to rationalise the orientation dependence of the remanence and the coercive force. The measured values are not very exact because of the rather small mass of specimen employed ($\sim$ 60 g). Indeed, the fit here is not good, although the correct trends are present, and for coercive force the coefficient A_0 is negative which is physically unreasonable. There is another possible source for the discrepancy between actual behaviour and theoretical prediction. For an exact application of Eq. (2), each grain should be subject to identical conditions e.g. constant, field or constant induction. In a typical polycrystal, however, the magnetic flux may be locally short-circuited along easy paths and avoid unfavourably oriented grains. Such behaviour is hard to quantify and its importance probably depends on the particular property under consideration.

CONCLUSIONS

Good agreement is obtained between measured torque magnetometer data and computed values based on orientation distributions derived from x-ray diffraction measurements.

Using orientation distribution data it is possible to analyse measured magnetic property data into orientation-dependent and orientation-independent components. For a.c. power loss values, the former contribution derives entirely from the normal hysteretic component. The classical eddy current loss and an anomalous loss of approximately the same value constitute the orientation-independent component. The analysis employed is quite general and may be used to obtain values of the desired physical property for a range of conditions.

ACKNOWLEDGMENTS

The authors are most grateful to Dr. R. O. Williams for making available the "Biaxial" computer program. They also thank the British Steel Corporation, Strip Mills Division, for financial assistance and for help with the testing of magnetic properties.

REFERENCES

1. P. N. Goss, *Trans. A.S.M.* **23**, 515, (1935).
2. R. M. Bozorth, *Ferromagnetism* (D. Van Nostrand, 1951), p. 778.
3. R. H. Pry and C. P. Bean, *J. Appl. Phys.* **29** (3), 532, (1958).
4. E. W. Lee, *Proc. I.E.E.* **105C**, 337, (1958).
5. K. J. Overshott, I. Preece and J. E. Thompson, *Proc. I.E.E.* **115**, 1840 (1968).
6. M. McCarty, G. L. Houze and F. A. Malagari, *J. Appl. Phys.* **38**, 1096 (1967).
7. M. R. Daniels, *I.E.E. Conf. Publ.* **33** (1967), pp. 4–8.
8. N. S. Akulov, *Z. Phys.* **54**, 582 (1929).
9. L. P. Tarasov and F. Bitter, *Phys. Rev.* **52**, 353 (1937).
10. R. O. Williams, *Trans. TMS-AIME* **242**, 105 (1968).
11. H. J. Bunge, *Z. Metallkunde* **56**, 872, (1965).
12. R.-J. Roe, *J. Appl. Phys.* **36**, 2024, (1965).
13. H. J. Bunge, *Mber. dtsch. Akad. Wiss.* **3**, 97 (1961).

14. H. J. Bunge, *Phys. Stat. Sol.* **26,** 167 (1968).
15. W. B. Hutchinson and J. G. Swift, to be published in *J. Pol. Acad. Sci.*
16. A. J. Heckler and W. G. Granzow, *Met. Trans.* **1,** 2089 (1970).
17. L. K. Jetter and B. S. Borie, *J. Appl. Phys.* **24,** 532,(1953).
18. I. L. Dillamore, C. J. E. Smith and T. W. Watson, *Met. Sci. J.*, **1,** 49 (1967).
19. I. L. Dillamore, P. L. Morris, C. J. E. Smith and W. B. Hutchinson, to be published in *Proc. Roy. Soc.*
20. P. L. Morris and W. B. Hutchinson, to be published.
21. Ref. 2, p. 567.